A New Photolabile Precursor of Glycine with Improved Properties: A Tool for Chemical Kinetic Investigations of the Glycine Receptor[†]

Christof Grewer,[‡,§] Jürgen Jäger,[‡,||] Barry K. Carpenter,[⊥] and George P. Hess*,[‡]

Department of Molecular Biology and Genetics, 217 Biotechnology Building, Cornell University, Ithaca, New York 14853-2703, and Department of Chemistry and Chemical Biology, Cornell University, Ithaca, New York 14853-1301

ABSTRACT: The synthesis and characterization of a new photolabile precursor of glycine (caged glycine) is described. The α-carboxyl group of glycine is covalently coupled to the α-carboxy-2-nitrobenzyl (αCNB) protecting group. Photolysis of the caged glycine with UV light produces free glycine. At 308 nm, the compound photolyzes with a quantum yield of 0.38. The absorption spectrum and the pH dependence of a transient absorption produced after laser-flash illumination are typical for *aci*-nitro intermediates of αCNB-protected compounds. The time constant for the major component of the *aci*-nitro intermediate decay (≈84% of the total *aci*-nitro absorbance) was determined to be 7 μs at physiological pH. A minor component (≈16%) decays with a rate constant of 170 μs. The compound does not activate or inhibit the α_1-homomeric glycine receptor transiently expressed in HEK293 cells. After photolysis with a 10 ns pulse of 325 nm laser light, the glycine released from the caged compound activates glycine-mediated whole-cell currents in the same cells. The rise of these currents can be measured in a time-resolved fashion and occurs on a millisecond to sub-millisecond time scale. It can be described with a single-exponential function over >85% of the total current. The rate constant of the current rise is about 2 orders of magnitude slower than the rate constant of caged glycine photolysis. Thermal hydrolysis of the αCNB-caged glycine takes place with a half-life of 15.6 h at physiological pH. The new caged glycine is the first in a series of photoprotected glycine derivatives that has the required properties for use with chemical kinetic methods for investigation of glycine-activated cell surface receptors. Photolysis is rapid and efficient with respect to the receptor reactions to be studied; hydrolysis in aqueous solution is sufficiently slow, and the compound is biologically inert. It will, therefore, be a useful tool for investigation of the processes leading to channel opening of glycine receptor channels and the effects of mutations of the glycine receptor and of inhibitors on these processes.

The functional bases of rapid chemical signal transmission between the 10^{12} neurons of the mammalian nervous system are the neurotransmitter receptors embedded in the postsynaptic membrane (*1*). These receptors transiently open transmembrane channels selective for small inorganic cations or anions after the binding of neurotransmitter that is secreted from the presynaptic cell. The associated ion flux across the postsynaptic cell membrane results in a change of the membrane potential of the postsynaptic cell which, with the correct sign and amplitude, can trigger signal transmission to other cells (*1*). If these receptor channels are selective for cations, opening changes the membrane potential to more positive values, leading to excitation which facilitates signal transmission. These receptors are activated by glutamate, serotonin, and acetylcholine. Activation of anion-selective channels changes the membrane potential to more negative values, leading to inhibition of signal transmission. The γ-aminobutyric acid ($GABA_A$) and glycine receptors belong to this class of ion channels (*2*).

The glycine receptor mediates inhibitory neurotransmission in the spinal cord and in the brain (*3*). It belongs to a superfamily of transmembrane proteins sharing similar structural features, including the nicotinic acetylcholine receptor and the $GABA_A$ receptor (*4, 5*). The native receptor is composed of α- and β-subunits (*6*). Several subtypes of the α-subunit have been characterized, including neonatal and adult subtypes. The glycine receptor is activated by glycine, β-alanine, and taurine and inhibited by strychnine (*6*). It is involved in malfunctions of the nervous system such as murine spastic disease (*7*) and human hyperekplexia (*8, 9*). It is a potential target for general anesthetics and alcohols (*10, 11*).

The time course of transient voltage changes at the postsynaptic membrane depends, among other factors, on the concentration of open channels in the cell membrane as a function of time and neurotransmitter concentration (*12, 13*).

* To whom correspondence should be addressed: 217 Biotechnology Building, Cornell University, Ithaca, NY 14853-2703. Telephone: (607) 255-4809. Fax: (607) 255-2428. E-mail: gph2@cornell.edu.

‡ Department of Molecular Biology and Genetics, Cornell University.

§ Current address: Max-Planck-Institute for Biophysics, Kennedyallee 70, D-60596 Frankfurt, Germany.

|| Current address: ARPIDA AG, Dammstrasse 36, CH-4142 Münchenstein, Switzerland.

⊥ Department of Chemistry and Chemical Biology, Cornell University.

This parameter, related to the kinetics of glycine receptor activation and desensitization, can be measured using rapid chemical kinetic techniques (*14*, *15*). Information about the kinetics of glycine receptor activation and desensitization has been obtained using single-channel recording experiments (*2*, *16*, *17*) and rapid solution exchange methods with outside-out membrane patches (*18*, *19*). However, because activation of rapid ligand-gated ion receptor channels typically takes place on a millisecond to sub-millisecond time scale (*12*, *20*), a technique with adequate time resolution, the laser-pulse photolysis technique, has been developed recently (*20*, *21*). This method utilizes caged precursors of neurotransmitters which can be photolyzed with a short UV light pulse to generate free neurotransmitter, typically within less than 50 μs (*22*).

Several caged glycine receptor ligands have been developed, including 1-[1-(4′,5′-dimethoxy-2′-nitrophenyl)ethyl]-glycine (*23*), a series of α-substituted *N*-caged 2-nitrobenzyl glycines (*24*), 2-methoxy-5-nitrophenyl glycine (MNP-glycine) (*25*), and MNP-β-alanine (*15*). Among these, the derivatives based on the *N*-caged 2-nitrobenzyl caging group have the disadvantage of low quantum yields and/or slow glycine release. MNP-glycine photolyzes within 3 μs and with a quantum yield of 0.2 (*25*), but it is not stable at neutral pH. It hydrolyzes with a half-life of 4.2 min (*15*) and is, therefore, not well suited for chemical kinetic experiments or studies in which the caged compound must be equilibrated with cell preparations for some length of time, for instance, in experiments designed to locate the position of neurotransmitter receptors by photolyzing the caged compounds in small areas of the cell surface and determining the response electrophysiologically (*26*−*28*). The MNP-β-alanine has the same photochemical properties as MNP-glycine but is more stable in aqueous solution. Its half-life for thermal hydrolysis at neutral pH is 100 min (*15*). This compound can be used in chemical kinetic experiments. However, β-alanine is only a partial agonist or competitive inhibitor when applied to some of the mutant human hyperekplexia receptors (*9*). Therefore, it is useful to have an improved photolabile glycine precursor available. Here we report the synthesis and characterization of a new caged glycine derivative utilizing the α-carboxy-2-nitrobenzyl (αCNB) protecting group (*21*) in the form of a glycine ester. This protecting group has been successfully used in the past to protect carbamoylcholine (carbamate linkage; *21*), glutamic acid (*29*), GABA (*30*), and kainic acid (*31*). All of these caged neurotransmitters liberate the neurotransmitter with a $t_{1/2}$ of <50 μs and with a quantum yield of >0.14 (reviewed in ref *13*). We show here that this caging group can be used to protect the carboxy function of glycine. The αCNB-glycine has favorable photochemical properties, comparable to those of other αCNB-protected carboxylic acids. It is stable at physiological pH, does not affect the function of the glycine receptor, and can be used to investigate glycine receptor activation, as shown here for the α1-homomeric glycine receptor expressed in HEK293 cells.

MATERIALS AND METHODS

The reaction scheme for the synthesis of α-carboxy-2-nitrobenzylglycine is given in Scheme 1.

2-Nitromandelic Acid 2. 2-Nitrobenzaldehyde **1** (4 g, 26.5 mmol) was dissolved in glacial acetic acid (30 mL) and KCN

Scheme 1
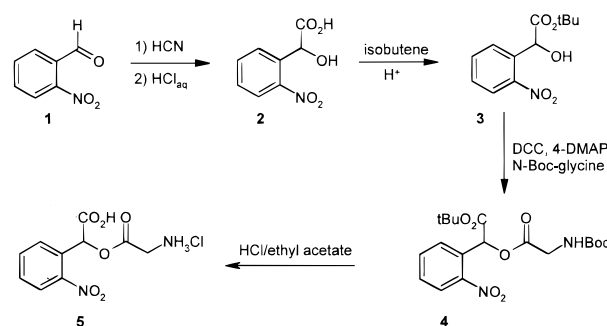
(3 g, 46 mmol), and 2 mL of water was added. The reaction flask was closed, and the mixture was stirred for 1.5 h at room temperature; then concentrated HClaq (50 mL) was added at once, and stirring was continued for 6 h at room temperature and for 8 h at 80 °C. The reaction was carried out with the necessary precautions (HCN is produced) in an efficient fume hood. The solvent was removed under reduced pressure and the residue extracted with ethyl acetate. The organic solution was washed with water and dried over MgSO4. The residue after evaporation of the solvent was recrystallized from ethyl acetate/hexane to give 4.8 g of **2** (24 mmol, 90%) as pale yellow crystals: mp 139 °C [lit. (*32*) 138−139 °C]; ^{1}H NMR (200 MHz, acetone-d_6) δ 8.0 (dd, 1H, J_1 = 1.3 Hz, J_2 = 8 Hz), 7.9 (dd, 1H, J_1 = 1.3 Hz, J_2 = 7.7 Hz, C$_6$H), 7.7 (dt, 1H, J_1 = 1.3 Hz, J_2 = 7.7 Hz, C$_5$H), 7.5 (dt, 1H, J_1 = 1.5 Hz, J_2 = 7.7 Hz, C$_4$H), 5.3 (bs, 1H, OH), 5.9 (s, 1H, CH).

tert-Butyl-2-nitromandelate 3. 2-Nitromandelic acid **2** (2 g, 10.1 mmol) was suspended in a mixture of CH$_2$Cl$_2$ (40 mL) and isobutene (10 mL) at −50 °C; 0.2 mL of H$_2$SO$_4$ was added, and the mixture was stirred for 8 h while warming to room temperature. After addition of 100 mL of diethyl ether, the solution was washed twice with 40 mL of saturated bicarbonate solution and dried over MgSO$_4$ before the solvent was removed under reduced pressure. The crude product was purified by column chromatography (silica gel, 3:7 ethyl acetate/petroleum ether, R_f = 0.7) to yield 1.52 g (6.0 mmol, 60%) of **3** as a pale yellow oil: ^{1}H NMR (200 MHz, CDCl$_3$) δ 7.96 (dd, 1H, J_1 = 8 Hz, J_2 = 1.2 Hz, C$_3$H), 7.49−7.74 (m, 3H, ArH), 5.85 (s, 1H, CH), 3.7 (bs, 1H, OH), 1.39 [s, 9H, C(CH$_3$)$_3$]; ^{13}C NMR (75.5 MHz, CDCl$_3$) δ 171.25 (CO$_2$), 133.74 (ArC−C), 133.45, 129.29, 129.18, 125.20 (C$_3$−C$_6$), 84.42 [$\underline{C}$(CH$_3$)$_3$], 69.96 (COH), 27.92 (CH$_3$).

α-*tert-Butyl-carboxylate-2-nitrobenzyl-N-Boc-glycine 4*. *tert*-Butyl 2-nitromandelate (0.75 g, 3 mmol), *N*-Boc-glycine (0.6 g, 3.4 mmol), and 10 mg of 4-(dimethylamino)pyridine (DMAP) were dissolved in 20 mL of CH$_2$Cl$_2$. DCC (3.5 mL, 1 M in CH$_2$Cl$_2$) was added, and the mixture was stirred for 2 h at room temperature; then diethyl ether (80 mL) was added, and the mixture was washed three times with 30 mL of saturated bicarbonate solution. The organic solution was dried over MgSO$_4$ before the solvent was removed under reduced pressure. The crude product was purified by column chromatography (silica gel, 3:7 ethyl acetate/petroleum ether, R_f = 0.6) to yield 840 mg of **4** (2 mmol, 69%) as colorless crystals: mp 100 °C; ^{1}H NMR (200 MHz, CDCl$_3$) δ 8.03 (d, 1H, J = 7.2 Hz, C$_3$H), 7.5−7.7 (m, 3H, ArH), 6.8 (s, 1H, CH), 5.04 (bs, 1H, NH), 4.1 (d, 2H, J = 5.6 Hz, CH$_2$), 1.44 [s, 9H, C(CH$_3$)$_3$], 1.4 [s, 9H, C(CH$_3$)$_3$]; ^{13}C NMR (75.5

MHz, CDCl$_3$) δ 169.13 (CO$_2$), 165.86 (CO$_2$), 148.07 (Ar C$-$NO$_2$), 133.46, 129.76, 129.08, 125.12 (C$_3$$-C_6$), 118.53 (Ar C$-$C), 83.84 [$\underline{C}$(CH$_3$)$_3$], 70.82 (Ar$-$C), 43.32 (CH$_2$), 28.26, 27.70 (CH$_3$). Anal. Calcd for C$_{19}H_{26}N_2O_6$: C, 55.60; H, 6.39; N, 6.83. Found: C, 55.39; H, 6.33; N, 6.82.

α-*Carboxy-2-nitrobenzyl-glycine Hydrochloride and* α*CNB-Glycine Hydrochloride* **5**. α-*tert*-Butyl-carboxylate-2-nitrobenzyl-*N*-Boc-glycine **4** (300 mg, 0.73 mmol) was dissolved in 3 mL of ethyl acetate, saturated with HCl. The solution was stirred for 3 h at room temperature, and then the solvent was removed under reduced pressure and the residue dried under high vacuum to yield 213 mg (0.73 mmol, 100%) of **5**: mp 179 °C; ^{1}H NMR (200 MHz, D$_2$O) δ 7.9 (d, 1H, J = 1.1 Hz, C$_3$H), 7.3$-$7.7 (m, 3H, ArH), 4.6 (s, 1H, CH), 3.9 (AB, 1H, J_{ab} = 7.6 Hz, CH$_a$$\underline{H}_b$), 3.8 (AB, 1H, J_{ab} = 7.6 Hz, C$\underline{H}_a$H$_b$); ^{13}C NMR (75.5 MHz, D$_2$O) δ 168.80 (CO$_2$), 164.25 (CO$_2$), 131.78, 128.07, 128.01, 122.73 (C$_3$$-C_6$), 125.68 (Ar C$-$C), 70.12 (Ar$-$C), 37.25 (CH$_2$). Anal. Calcd for C$_{10}H_{11}ClN_2O_6$: C, 41.32; H, 3.81; N, 9.64. Found: C, 41.73; H, 4.06; N, 9.31.

Laser-Flash Photolysis. Transient absorption experiments were performed as described previously (*21*). The 308 nm light output of a XeCl excimer laser (Lumonics TE861, 50 mJ primary output, 10 ns pulse duration) was used to illuminate a 2 mm $\times$ 2 mm $\times$ 10 mm quartz cuvette containing the sample solution. The absorption change after laser excitation was measured with the light of a halogen lamp (Newport 780) passing through the cuvette perpendicular to the laser beam. The path length of the analysis light was 10 mm. The wavelength of the analysis light was selected with a monochromator (McPherson 275) and the light intensity measured with a photomultiplier (Thorn EMI 9635QB). The signal of the photomultiplier was preamplified (Thorn EMI model A1) and recorded with a digital oscilloscope (LeCroy Scope Station 140). The quantum yield was determined as described previously (*21*). The absorbance, A_n, of the *aci*-nitro intermediate was measured as a function of the number of consecutive laser pulses, *n*. The solution was stirred between laser flashes. Assuming that the absorbance, and therefore the concentration of the *aci*-nitro intermediate, is directly proportional to the concentration of the liberated compound (*33$-$36*) and that the absorbance of the solution does not change during the experiment (irradiation near the isosbestic point; *33*), the quantum yield ϕ can be determined using the following equation (*21*):

$$A_n = \epsilon_M L C_0 \phi K_E \exp[-\phi K_E F(n-1)] \qquad (1)$$

where ϵ_M represents the molar extinction coefficient of the *aci*-nitro intermediate, L represents the path length of the analysis light, C_0 is the initial concentration of the caged compound, K_E is the ratio of absorbed photons to the number of molecules in the irradiated volume, F is the fraction of the solution irradiated, and n is the number of laser pulses. The quantum yield ϕ can be calculated from the slope of a semilogarithmic plot of the absorbance versus $n-1$ (eq 1). The extinction coefficient of the *aci*-nitro intermediate is obtained from the intercept (*21*). The experiments described above were performed at pH 7.3 in 100 mM phosphate buffer.

Cell Experimentation. The cDNA encoding the α_1-subunit of the human glycine receptor (*37*) in a pCIS construct for mammalian expression (*38*) was kindly provided by H. Betz (Frankfurt, Germany). Exponentially growing HEK293 cells were transfected with the glycine receptor DNA using Superfect transfection reagent (Qiagen). Cells were then used for whole-cell current recording 2$-$4 days after transfection. HEK293 cells were cultured as described (ATTC). Transfected cells were detected by fluorescence of coexpressed green fluorescent protein (GIBCO pGreenLantern). Whole-cell currents were recorded as described previously (*39*). The recording pipet solution contained 120 mM CsCl, 2 mM MgCl$_2$, 10 mM TEACl, 10 mM EGTA, and 10 mM HEPES adjusted to pH 7.3, and the bath buffer solution contained 140 mM NaCl, 5 mM KCl, 1 mM MgCl$_2$, 2 mM CaCl$_2$, 10 mM HEPES, and 10 mM glucose adjusted to pH 7.3. Transmembrane potentials were corrected for liquid junction potentials (*40*). Typical pipet resistances were 2.5$-$3.5 MΩ, and the series resistance was 5$-$6 MΩ. Whole-cell currents were corrected for series resistance errors to up to 90%. Cell-flow experiments were performed as described by Udgaonkar and Hess (*41*). A cell-flow device (*42*) was used to rapidly exchange extracellular solutions. Whole-cell currents induced by rapid application of glycine to cell surface receptors were amplified with an Adams & List EPC-7 amplifier, low pass filtered at 1$-$10 kHz (Krohn-Hite 3322), and digitized with a Labmaster TL-1 (Scientific Solutions) digitizer board at 200$-$500 Hz which was controlled by software (Axon pClamp).

Laser-Pulse Photolysis. The laser light was provided by a Lumonics TE 861 excimer laser [XeCl, 308 nm; N$_2$, 337 nm; or the laser dye PTP (Lambda Physics), 342 nm] and was coupled by focusing with a 2 cm focal length quartz lens into a 300 μm diameter optical fiber (FiberGuide Industries), which delivered the laser light to the cell. Typical laser energies were 50$-$400 mJ/cm^2 as measured with an energy meter (Gentec ED-200) at the fiber output. The diameter of the illuminated area was 350$-$400 μm, large enough to prevent changes of the neurotransmitter concentration by diffusion during the time scale of the experiment of 50$-$100 ms. The concentration of the caged compound that was used was 500 μM to 1 mM. The amount of neurotransmitter released was controlled by adjusting the laser energy with neutral density filters and calibrated using the cell-flow method with known concentrations of glycine. The flash$-$flow system was controlled using the pClamp software (Axon Instruments). Data were sampled at 5$-$100 kHz and filtered at 5$-$50 kHz.

Data Analysis. Linear and nonlinear regression (Marquardt algorithm) as well as plotting was performed using Origin software (MicroCal).

RESULTS

A number of criteria determine the suitability of a new caged neurotransmitter for rapid chemical kinetic investigations of neurotransmitter receptors on cell surfaces. Among these are (i) the rate constant of neurotransmitter release, (ii) the quantum yield of photolysis, (iii) the inertness with respect to the receptor reactions to be studied, (iv) the solubility in aqueous solution, and (v) the stability in aqueous solution at physiological pH (*43*). How does the new αCNB-caged glycine meet these specifications? The answer to this question is discussed below.

Rate Constant and Quantum Yield of Photolysis. The rate constant of glycine release was estimated by measuring the rate constant of the *aci*-nitro intermediate decay. There is evidence that the *aci*-nitro intermediate decay leads to the formation of the free neurotransmitter (*35, 36*). After a solution of caged glycine was excited with a pulse of 308 nm laser light, the absorbance of the *aci*-nitro intermediate was measured as a function of time (Figure 1a). The transient absorbance decays with two exponential components. About $74 \pm 6\%$ of the absorption decays with a $t_{1/2}$ of 4.6 ± 1 μs; $14 \pm 9\%$ decays with a $t_{1/2}$ of 125 ± 60 μs, and $12 \pm 8\%$ of the absorption is contributed by a steady state component caused by the absorption of the nitroso byproduct. These results are typical for neurotransmitters protected as αCNB esters (*29, 31*). The rate constants measured for **5** are about 200 times faster than the rate constants for liberation of glycine from the *N*-protected αCNB-glycine (*24*). Similar results have been obtained for caged glutamic acid in a comparison of the ester and amine linkages (*29*). To determine if the transient absorbance change is caused by the *aci*-nitro intermediate, we assessed the spectral dependence of the transient absorption. The spectrum recorded at different times after the laser flash is shown in the inset of Figure 1a. It is typical for *aci*-nitro intermediates, with an absorbance maximum near 430 nm (*33, 34*). The spectrum does not change within the first 20 μs of *aci*-nitro intermediate formation, suggesting that the fast and the slow component have similar spectral distributions (*29, 31*). The decay rate constant of the fast *aci*-nitro component was measured as a function of pH (Figure 1b). The rate constant decreases with increasing pH. This is typical for *aci*-nitro intermediates of αCNB-protected compounds (*21, 44*).

The quantum yield of caged glycine photolysis was determined using the method published by Milburn et al. (*21*). The absorbance A_n was measured as a function of the number of consecutive laser flashes and plotted in a semilogarithmic fashion according to eq 1 as shown in Figure 2. The quantum yield can be determined from the slope calculated by linear regression analysis as 0.38 ± 0.06. The quantum yield of glycine release is, therefore, approximately 20 times higher than the quantum yield of the corresponding compound with the amine linkage (*24*). Similar results have been reported for caged glutamic acid by comparing the ester and the amine linkage (*29*). The molar extinction coefficient of the *aci*-nitro intermediate was determined to be 1010 ± 240 M^{-1} cm^{-1} (435 nm, pH 7.3).

Stability in Aqueous Solution. The stability of caged glycine was tested using α_1-glycine receptor-transfected HEK293 cells as a highly sensitive glycine detector. The concentration of free glycine in a 1.3 mM solution of caged glycine was measured as a function of time after solubilization (Figure 3). A concentration of caged precursor typically used in chemical kinetic experiments is 1.3 mM. The initial concentration of glycine in the sample is 8 μM, which corresponds to a background of free glycine of 0.7%. The free glycine concentration increases with time as shown in Figure 3. The reaction was followed up to 160 min. The half-life of the hydrolysis reaction can be estimated to be about 15.6 h. The UV−visible spectrum of caged glycine did not change within 20 h, indicating that (i) the observed reaction was caused by thermal hydrolysis and not by photolysis related to background light and (ii) UV−visible
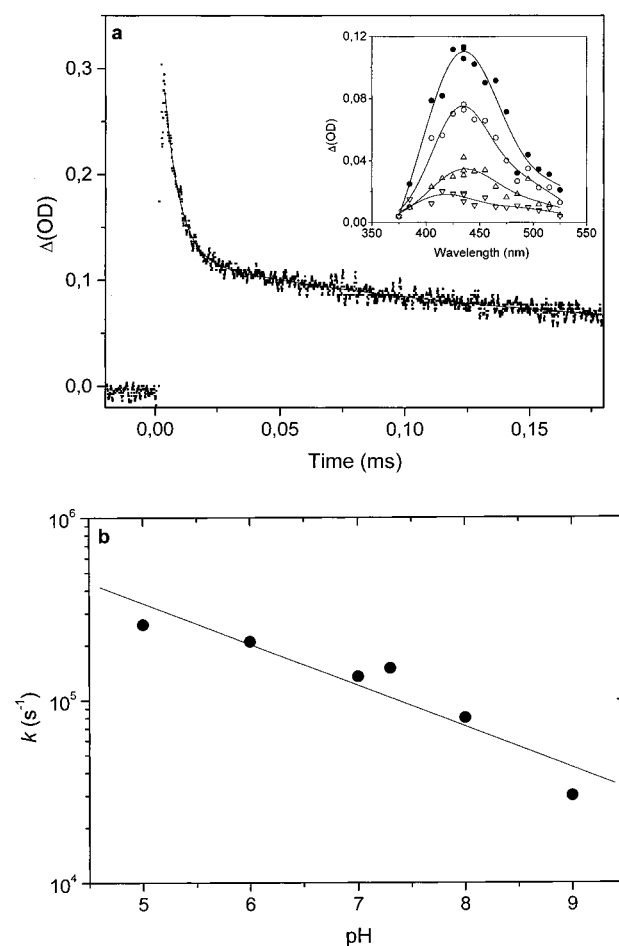

FIGURE 1: (a) Transient absorption of the *aci*-nitro intermediate at 435 nm. αCNB-caged glycine (1 mM) was photolyzed at time zero with a pulse of 308 nm laser light. The path length of the laser light path was 2 mm; the analyzing light path length was 10 mm. A total volume of 50 μL was irradiated. The incident laser energy was 19 mJ. The solid line represents a fit to a biexponential decay function plus a steady state absorption component. The fast component decays with an average time constant of 6.7 ± 1.5 μs and has a contribution to the total absorption of 0.74 ± 0.06. The slow component decays with an average time constant of 170 ± 80 μs and has a contribution to the total absorption of 0.14 ± 0.09. The steady state component has a contribution to the total absorption of 0.12 ± 0.08. The conditions of the experiment were as follows: 22 °C, 100 mM phosphate buffer, and pH 7.3. The inset shows the transient absorption spectrum induced by laser-flash photolysis of 1 mM αCNB-caged glycine. The transient absorption spectrum is typical for *aci*-nitro intermediates of αCNB-caged compounds. Spectra were recorded (from top to bottom) 1, 5, 20, and 500 μs after photolysis, showing that the 435 nm transient has fully decayed after 500 μs. The laser energy was 10 mJ. (b) The *aci*-nitro intermediate decay rate of αCNB-glycine, determined from the half-life values of the fast component of the decay function observed at 435 nm, is plotted as a function of the pH at 22 °C. The concentration of the caged glycine was 1 mM. The αCNB-caged glycine was photolyzed with a XeCl excimer laser at 308 nm. The incident laser energy was 20 mJ. The laser light path was 2 mm and the analyzing light path 10 mm. A total volume of 70 μL was irradiated. Buffer solutions were acetate (pH 5.0), phosphate (pH 6, 7, or 8), and borate (pH 9). The buffer concentrations were 100 mM.

spectrophotometry is not useful for the determination of the hydrolysis rate constant. In a comparison of αCNB-glycine with MNP-caged glycine receptor agonists, it is more stable than MNP-glycine by a factor of about 145 and more stable than MNP-β-alanine by a factor of about 10. The stability
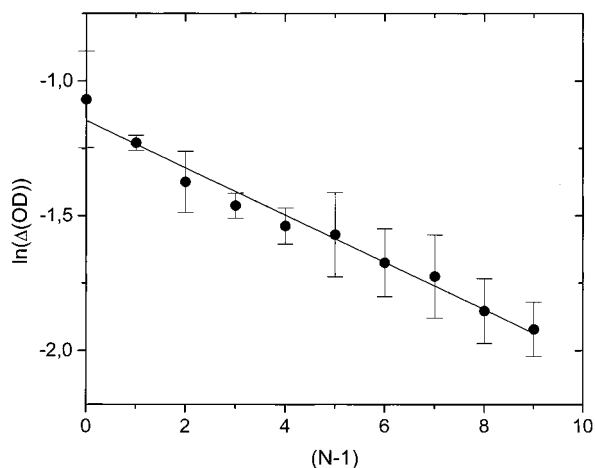
FIGURE 2: Determination of the photolysis quantum yield. Fifty microliters of a total volume of 80 μL of 2 mM caged glycine was photolyzed in a 2 mm $\times$ 10 mm cuvette with consecutive 22 mJ, 308 nm laser flashes. Nineteen millijoules of laser light was absorbed by the solution. The number of absorbed photons changed by less than 5% during the experiment. The solution was stirred after each laser flash. The maximum transient absorbance change was measured and plotted as a function of the number of laser flashes $-$ 1. From the slope, the quantum yield was determined to be 0.38 $\pm$ 0.06 (average value from four experiments). The slope was corrected for the change of the number of absorbed photons measured for each flash. The extinction coefficient for the *aci*-nitro intermediate was determined to be 1010 $\pm$ 240 M^{-1} cm^{-1}. The conditions of the experiment were as follows: 100 mM phosphate buffer, pH 7.3, and 22 °C.
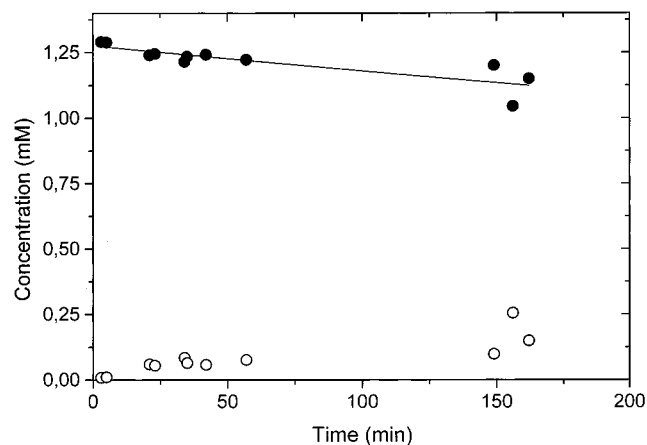

FIGURE 3: Amount of free glycine measured as a function of time after solubilization of 1.3 mM caged glycine. αCNB-glycine was kept in the dark for the period of the experiment. The white symbols represent data for free glycine; the black symbols represent data for caged glycine. The concentration of the caged precursor was calculated by subtracting the concentration of free glycine from the known initial concentration of caged glycine (1.3 mM). The solid line represents an estimate of the αCNB-glycine hydrolysis calculated with a $t_{1/2}$ of 15.6 h. The spectrum of the αCNB-glycine did not change within 20 h. The free glycine concentration was measured using glycine receptor-containing HEK293 cells as a detector together with the cell-flow method. The conditions of the experiment were as follows: pH 7.3 and 22 °C.

in aqueous solution is similar to the stability of αCNB-glutamate caged at the α-carboxy function (*29*).

Photolysis of Caged Glycine Activates Glycine Receptors. Photolysis of caged glycine activates a whole-cell current in HEK293 cells transfected with α_1-glycine receptor cDNA (Figure 4a, left panel). In this experiment, the cell attached to a recording electrode in the whole-cell configuration was
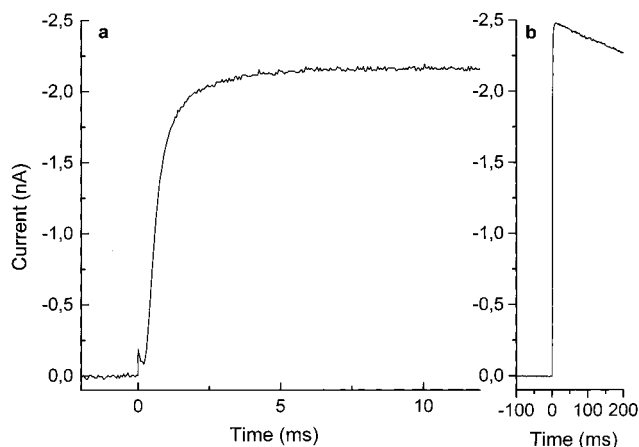

FIGURE 4: (a) Glycine receptor activation caused by photolytic release of glycine from αCNB-caged glycine. αCNB-caged glycine (1 mM) was passed over the cell surface of HEK293 cells transfected with α_1-glycine receptor cDNA for 500 ms. At time zero, the solution flow was stopped and the laser was fired. The concentration of the glycine that was released was 240 μM, calibrated using the cell-flow method with 1 mM glycine as shown in panel b. The current rise can be described by a sum of two exponentials with a τ_1 of 550 $\pm$ 20 μs (90% of the total current) and a τ_2 of 4.3 $\pm$ 0.4 ms (10% of the total current). The conditions of the experiment were as follows: 22 °C, $-$60 mV, and pH 7.3.

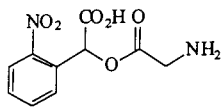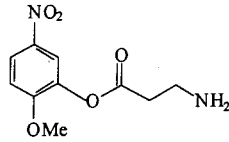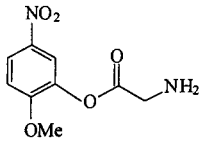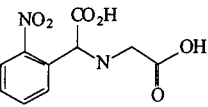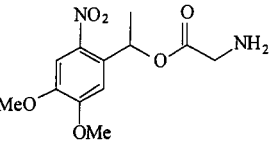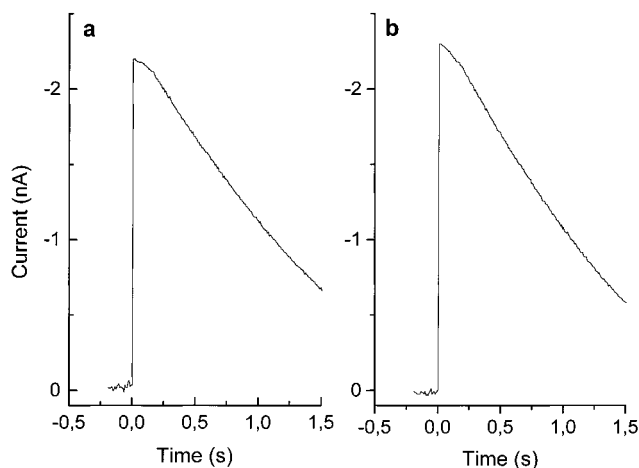FIGURE 5: αCNB-caged glycine does not inhibit the glycine receptor. Glycine (1 mM) was passed over the surface of HEK293 cells transfected with α_1-glycine receptor cDNA in the absence (a) and presence (b) of 1 mM αCNB-caged glycine, and the glycine-induced current was recorded in the whole-cell configuration. The conditions of the experiment were as follows: 22 °C, $-$60 mV, and pH 7.3.

equilibrated with 1 mM caged glycine for 500 ms before photolysis was initiated at time zero. No activation of a whole-cell current is observed until the compound is photolyzed. After photolysis, the current rises rapidly to reach a plateau value at about 7 ms. A single-exponential function is representative of the current rise for 90% of the total current according to the following equation (*20*):

$$I_t = I_{max}[1 - \exp(-k_{obs}t)] \qquad (2)$$

where I_t represents the observed whole-cell current at time t, I_{max} is the maximum whole-cell current in the absence of desensitization, and k_{obs} is the observed pseudo-first-order rate constant of the current rise. The rate constant of the current rise k_{obs} was determined to be 1820 $\pm$ 70 s^{-1}. A

Table 1: Photochemical Properties of Caged Ligands of the Glycine Receptor

Compound	Photolysis $t_{1/2}$ [μs]	Quantum yield	Hydrolysis $t_{1/2}$ [min]	Reference
αCNB-glycine ester	4.6	0.38	940[a]	
MNP-β-alanine	< 3	0.2	100[b]	(15)
MNP-glycine	< 3	0.2	4.2[b]	(25)
N-(αCNB)glycine	2300	0.02	-	(24)
1-[1-(4',5'-dimethoxy-2'nitrophenyl)ethyl]glycine	10^6	-	-	(23)

[a] pH 7.3. [b] pH 7.1 (15).

minor, slow, component with a rate constant k_{obs} of 230 ± 20 s^{-1} contributes about 10% to the total current. The reason for the two exponential components in the current rise is not known. It has not been observed with native glycine receptors in mouse spinal cord and rat hippocampal neurons (15, 24). The cell-flow method was used to calibrate the concentration of glycine released by the laser flash (Figure 4b, right panel). Glycine (1 mM) flowed over the surface of the same cell that was used for the photolysis experiment whose results are depicted in Figure 4a. Similar cell-flow experiments at different glycine concentrations (45), together with published values for the apparent dissociation constant for dissociation of glycine from the receptor (18−30 μM; 46, 47), provided the basis for estimating the concentration of glycine released from 1 mM caged glycine in the photolysis experiment whose results are depicted in Figure 4a as 240 μM. This result shows that glycine at concentrations high enough to saturate the glycine-binding sites of the α₁-homomeric receptor can be released from the caged precursor.

Results from additional control experiments are shown in Figure 5. Glycine was passed over the cell surface in the absence (Figure 5a) and presence (Figure 5b) of 1 mM caged glycine. The whole-cell current is not decreased in the presence of caged glycine, indicating that the receptor is not inhibited by the caged precursor in this time domain. The receptor is also not activated by αCNB-caged glycine at concentrations up to 2 mM. These experiments indicate that αCNB-glycine is biologically inert.

DISCUSSION

The potential of the αCNB group for protecting carboxylic acids has been shown in the past for compounds such as glutamic acid (29), GABA (30), and kainic acid (31). It is now shown in this work that this group is also very useful for caging glycine, an important neurotransmitter which activates the glycine receptor. This new compound adds to the series of compounds demonstrating the usefulness of the αCNB caging group, especially for protecting the carboxy function of biologically important compounds. The new

caged glycine was synthesized from readily available starting materials (Scheme 1). It is the first in a series of previously synthesized caged glycine derivatives that meet the desired prerequisites for successful use in chemical kinetic experiments for investigation of glycine receptor activation. These desirable properties are a high rate of photolysis with respect to the rate constants of the glycine-mediated receptor reactions, a satisfactory quantum yield, biological inertness, and a sufficient stability in aqueous solution. Photolysis activates α_1-glycine receptor-mediated currents in HEK293 and thus demonstrates the usefulness of this compound for transient kinetic investigations of the glycine receptor in cell membranes in the microsecond to millisecond time domain. The caged precursor does not activate whole-cell currents in the same cells. The properties of the caged glycine receptor ligands are summarized in Table 1. Together with the MNP-β-alanine (*15*), two caged glycine receptor ligands are now available which allow the chemical kinetic investigation of wild type and mutant glycine receptors.

It is shown here that glycine induces whole-cell currents mediated by α_1-homomeric glycine receptors which rise with a time constant in the millisecond to sub-millisecond time domain, at subsaturating glycine concentrations. The necessary time resolution is easily achieved with the laser-pulse photolysis method using the new αCNB-glycine ester but not with rapid solution exchange methods. The time resolution for the cell-flow method has been estimated to be about 20 ms (*41*) when used with whole cells. Rapid solution exchange methods have been also applied to the investigation of receptor channel activation in outside-out membrane patches (*48*). When concentrations of activating ligands are far in excess of the concentrations necessary to saturate the receptor, the time resolution of the method will improve because a small concentration, sufficient to activate the receptor, will reach the cell surface receptors in a time that is short compared to the time needed for total solution exchange (*48*). This has two implications. (i) The number of receptors in a membrane patch is at least 100-fold smaller than the number of receptors in a whole cell; thus, the current will be reduced by the same factor. It will be, therefore, difficult to detect minor components of the current rise as shown here for the α_1-homomeric glycine receptor, or heterogeneity in receptor populations as demonstrated before for native glycine receptors in spinal cord neurons (*14*). (ii) When using supersaturating concentrations of activating ligand, information about processes occurring at intermediate to low ligand concentrations cannot be obtained. Therefore, only limiting values of the rate constants pertaining to the receptor channel activation process can be measured.

The availability of a new, improved caged glycine with desirable photochemical and biological properties makes it now possible to determine properties of glycine receptors that could not be investigated with conventional rapid solution exchange methods. It will now be possible to determine the effects of glycine concentration on the rate constants of the receptor channel activation process, providing further information about the details of the underlying kinetic mechanism. With laser-pulse photolysis of this caged glycine, the rate constants of channel opening, at high glycine concentrations, and closing, at intermediate glycine concentrations, of glycine receptors can be measured independently. From these experiments, it will be possible to determine the maximum likelihood of receptor channels being open. At low ligand concentrations, the rate constants for formation of the ligand−receptor complex can be measured. Furthermore, the effect of glycine receptor inhibitors, such as strychnine (*49*), and potentiators such as ethanol (*11*) and Zn^{2+} (*50*) on the rate constants for channel opening and closing can be determined. This will provide information about the mechanism of modulator−receptor interaction, as has been shown earlier for the acetylcholine receptor (*51−54*). In addition, it will be possible to obtain detailed information about how single amino acid mutations, such as the startle disease mutations (*8*), affect the rate and equilibrium constants of ligand binding and receptor channel opening. The αCNB-caged glycine will add to the MNP-β-alanine (*15*) as a useful tool for studying glycine receptor function.

REFERENCES

1. Kandel, E. R., Schwartz, J. H., and Jessel, T. M. (1995) *Essentials of Neural Sciences and Behavior*, Appleton & Lange, East Norwalk, CT.
2. Bormann, J., Hamill, O. P., and Sakmann, B. (1987) *J. Physiol. 385*, 243−286.
3. Aprison, M. H., and Daly, E. (1978) *Adv. Neurochem. 3*, 203−294.
4. Betz, H. (1990) *Neuron 5*, 383−392.
5. Stroud, R. M., McCarthy, M. P., and Shuster, M. (1990) *Biochemistry 29*, 11009−11023.
6. Langosch, D., Becker, C. M., and Betz, H. (1990) *Eur. J. Biochem. 194*, 1−8.
7. Becker, C. M., Schmieden, V., Tarroni, P., Strasser, U., and Betz, H. (1992) *Neuron 8*, 283−289.
8. Shiang, R., Ryan, S. G., Zhu, Y. Z., Hahn, A. F., O'Connell, P., and Wasmuth, J. J. (1993) *Nat. Genet. 5*, 351−358.
9. Rajendra, S., Lynch, J. W., Pierce, K. D., French, C. R., Barry, P. H., and Schofield, P. R. (1994) *J. Biol. Chem. 269*, 18739−18742.
10. Jones, M. V., and Harrison, N. L. (1993) *J. Neurophysiol. 70*, 1339−1349.
11. Mascia, M. P., Machu, T. K., and Harris, R. A. (1996) *Br. J. Pharmacol. 119*, 1331−1336.
12. Hess, G. P. (1993) *Biochemistry 32*, 989−1000.
13. Hess, G. P., and Grewer, C. (1998) *Methods of Enzymology*, Vol. 291, Academic Press, San Diego.
14. Walstrom, K. M., and Hess, G. P. (1994) *Biochemistry 33*, 7718−7730.
15. Niu, L., Wieboldt, R., Ramesh, D., Carpenter, B. K., and Hess, G. P. (1996) *Biochemistry 35*, 8136−8142.
16. Takahashi, T., Momiyama, A., Hirai, K., Hishinuma, F., and Akagi, H. (1992) *Neuron 9*, 1155−1161.
17. Twyman, R. E., and Macdonald, R. L. (1991) *J. Physiol. 435*, 303−332.
18. Legendre, P. (1998) *J. Neurosci. 18*, 2856−2870.
19. Harty, T. P., and Manis, P. B. (1998) *J. Neurophysiol. 79*, 1891−1901.
20. Matsubara, N., Billington, A. P., and Hess, G. P. (1992) *Biochemistry 31*, 5507−5514.
21. Milburn, T., Matsubara, N., Billington, A. P., Udgaonkar, J. B., Walker, J. W., Carpenter, B., Webb, W. W., Marque, J., Denk, W., McCray, J. A., and Hess, G. P. (1989) *Biochemistry 28*, 49−56.
22. Hess, G. P., Niu, L., and Wieboldt R. (1995) *Ann. N.Y. Acad. Sci. 757*, 23−39.

23. Wilcox, M., Viola, R. W., Johnson, K. W., Billington, A. P., Carpenter, B. K., McCray, J. A., Guzikowski, A. P., and Hess, G. P. (1990) *J. Org. Chem. 55*, 1585−1589.

24. Billington, A. P., Walstrom, K. M., Ramesh, D., Guzikowski, A. P., Carpenter, B. K., and Hess, G. P. (1992) *Biochemistry 31*, 5500−5507.

25. Ramesh, D., Wieboldt, R., Niu, L., Carpenter, B. K., and Hess, G. P. (1993) *Proc. Natl. Acad. Sci. U.S.A. 90*, 11074−11078.

26. Denk, W., Delaney, K. R., Gelperin, A., Kleinfeld, D., Strowbridge, B. W., Tank, D. W., and Yuste, R. (1994) *J. Neurosci. Methods 54*, 151−162.

27. Katz, L. C., and Dalva, M. B. (1994) *J. Neurosci. Methods 54*, 205−218.

28. Li, H., Avery, L., Denk, W., and Hess, G. P. (1997) *Proc. Natl. Acad. Sci. U.S.A. 94*, 5912−5916.

29. Wieboldt, R., Gee, K., Ramesh, D., Carpenter, B. K., and Hess, G. P. (1994) *Proc. Natl. Acad. Sci. U.S.A. 91*, 8752−8756.

30. Gee, K. R., Wieboldt, R., and Hess, G. P. (1994) *J. Am. Chem. Soc. 116*, 8366−8367.

31. Niu, L., Gee, K. R., Schaper, K., and Hess, G. P. (1996) *Biochemistry 35*, 2030−2036.

32. McKenzie, A., and Steward, P. A. (1934) *J. Chem. Soc.*, 104−111.

33. McCray, J. A., Herbette, L., Kihara, T., and Trentham, D. R. (1980) *Proc. Natl. Acad. Sci. U.S.A. 77*, 7237−7241.

34. Schupp, H., Wong, W. K., and Schnabel, W. (1987) *J. Photochem. 36*, 85−97.

35. Walker, J. W., Reid, G. P., McCray, J. A., and Trentham, D. R. (1988) *J. Am. Chem. Soc. 110*, 7170−7177.

36. Wootton, J. F., and Trentham, D. R. (1989) *NATO Adv. Study Inst. Ser., Ser. C 272*, 277−296.

37. Grenningloh, G., Schmieden, V., Schofield, P. R., Seeburg, P. H., Siddique, T., Mohandas, T. K., Becker, C.-M., and Betz, H. (1990) *EMBO J. 9*, 771−776.

38. Gorman, C. M., Gies, D. R., McCray, G., and Huang, M. (1989) *Virology 171*, 377−385.

39. Hamill, O. P., Marty, A., Neher, E., Sakmann, B., and Sigworth, F. J. (1981) *Pfluegers Arch. 391*, 85−100.

40. Barry, P. H., and Lynch, J. W. (1991) *J. Membr. Biol. 121*, 101−117.

41. Udgaonkar, J. B., and Hess, G. P. (1987) *Proc. Natl. Acad. Sci. U.S.A. 84*, 8758−8762.

42. Krishtal, O. A., and Pidoplichko, V. I. (1980) *Neuroscience 5*, 2325−2327.

43. Adams, S. R., and Tsien, R. Y. (1993) *Annu. Rev. Physiol. 55*, 755−783.

44. Ramesh, D., Wieboldt, R., Billington, A. P., Carpenter, B. K., and Hess, G. P. (1993) *J. Org. Chem. 58*, 4599−4605.

45. Grewer, C. (1999) *Biophys. J. 77*, 727−738.

46. Bormann, J., Rundström, N., Betz, H., and Langosch, D. (1993) *EMBO J. 12*, 3729−3737.

47. Lynch, J. P., Rajendra, S., Pierce, K. D., Handford, C. H., Barry, P. H., and Schofield, P. R. (1997) *EMBO J. 16*, 110−120.

48. Liu, Y., and Dilger, J. B. (1991) *Biophys. J. 60*, 424−432.

49. Vandenberg, R. J., French, C. R., Barry, P. H., Shine, J., and Schofield, P. R. (1992) *Proc. Natl. Acad. Sci. U.S.A. 89*, 1765−1769.

50. Laube, B., Kuhse, J., Rundström, N., Kirsch, J., Schmieden, V., and Betz, H. (1995) *J. Physiol. 483*, 613−619.

51. Niu, L., and Hess, G. P. (1993) *Biochemistry 32*, 3831−3885.

52. Niu, L., Abood, L. G., and Hess, G. P. (1995) *Proc. Natl. Acad. Sci. U.S.A. 92*, 12008−12012.

53. Grewer, C., and Hess, G. P. (1999) *Biochemistry 38*, 7837−7846.

54. Jayaraman, V., Usherwood, P. N. R., and Hess, G. P. (1999) *Biochemistry 38*, 11406−11414.